UDC 534:519.6:62-413

Ivo SENJANOVIĆ[1]
Nikola VLADIMIR[1]
Neven HADŽIĆ[1]
Dae-Seung CHO[2]

Shear Locking-Free Finite Element Formulation for Thick Plate Vibration Analysis

Authors' addresses:
[1] *University of Zagreb, Faculty of Mechanical Engineering and Naval Architecture,* Ivana Lučića 5, 10000 Zagreb, Croatia
e-mail: ivo.senjanovic@fsb.hr
[2] *Pusan National University,* San 30 Jangjeon-dong, Guemjeong-gu, Busan, 609-735, Korea
Received (Primljeno): 2013-01-29
Accepted (Prihvaćeno): 2013-01-31
Open for discussion (Otvoreno za raspravu): 2014-09-30

Original scientific paper

The basic equations of the Mindlin thick plate theory are specified as starting point for the development of a new thick plate theory in which total deflection and rotations are split into pure bending deflection and shear deflection with bending angles of rotation, and in-plane shear angles. The equilibrium equations of the former displacement field are condensed into one partial differential equation for flexural vibrations. In the latter case two differential equations for in-plane shear vibrations are obtained and they are similar to the well-known membrane equations. Physical background of the derived equations is analysed in case of a simply supported square plate. Rectangular shear locking-free finite element for flexural vibrations is developed. For in-plane shear vibrations ordinary membrane finite elements can be used. Natural modes of plate layers in in-plane shear vibrations are the same as membrane modes, while natural frequencies have to be transformed. Application of the presented theory is illustrated in a case of simply supported and clamped square plate. Problems are solved analytically and by FEM. The obtained results, compared with the relevant ones available in literature, are discussed.

Keywords: *finite element method, flexural vibrations, Mindlin theory, shear locking, shear vibrations, thick plate*

Formulacija konačnih elemenata za analizu vibracija debele ploče bez smične blokade

Izvorni znanstveni rad

Navedeni su osnovni izrazi Mindlinove teorije debele ploče, kao polazna točka za razvoj nove teorije, u kojoj su ukupni progib i zakreti rastavljeni u progib čistoga savijanja i poprečnoga smicanja s kutovima zakreta savijanja i kutovima ravninskoga smicanja. Jednadžbe ravnoteže unutarnjih i izvanjskih sila prvoga polja pomaka reducirane su na jednu parcijalnu diferencijalnu jednadžbu fleksijskih vibracija. Za drugo polje pomaka dobivene su dvije diferencijalne jednadžbe za ravninsko smično vibriranje. Dinamičko ponašanje ploče opisano izvedenim jednadžbama analizirano je u slučaju slobodno oslonjene kvadratne ploče. Izveden je pravokutni konačni element za fleksijske vibracije ploče bez smične blokade. Za ravninsko smično vibriranje ploče korištena je analogija s membranskim vibracijama. Njihovi prirodni oblici su isti, dok se prirodne frekvencije membrane prenose na ploču pomoću jednostavnog izraza. Primjena razvijene teorije ilustrirana je na primjeru slobodno oslonjene i upete kvadratne ploče. Problem je riješen analitički i numerički metodom konačnih elemenata. Dobiveni rezultati uspoređeni su s objavljenim rezultatima, koji su određeni nekom drugom metodom na osnovi Mindlinove teorije.

***Ključne riječi*:** debela ploča, fleksijske vibracije, metoda konačnih elemenata, Mindlinova teorija, smična blokada, smične vibracije

1 Introduction

Thick plate is a structural element in many engineering structures. Double bottom, double skin and transverse bulkheads in ordinary ships, tankers and container ships, respectively, can be considered as an orthotropic thick plate. Also, thick plate is used as engine foundation, elements of reinforced concrete bridges, floating structures (airports, artificial recreating islands, pontoons), ice floe etc.

The first works on the thick plate theory are those of Reissner and Mindlin from 1945 and 1951, [1] and [2], respectively. This challenging problem has been a subject of investigation by many researchers, both mathematicians and engineers. A very large number of concepts have been worked out during that long period [3]. Analytical and numerical methods have been applied. When the finite element method (FEM) came into use, thanks to the development of computers, is was also applied for thick plate static and dynamic analysis [4].

In the Mindlin thick plate theory shear deformations are taken into account, and application of ordinary low-order finite element is not capable to reproduce the pure bending modes in the limit case of thin plate. This shear locking problem arises due to inadequate dependence among transverse deflection and two rotations. In order to overcome this problem, quite a large number of procedures have been developed in recent years. Most of them utilize a mixed formulation, by linking plate deflection field to the angles of rotations [5, 6, 7]. These formulations are rather complex and time consuming. Another method is the Assumed Natural Strain (ANS) in which shear strains at discrete collocation points are determined from the displacements and interpolated over the element surface with specific shape functions [8, 9, 10]. The Discrete Shear Gap method (DSG) is similar to the ANS since the course of certain strains is modified within the finite element [11]. The lack of collocation points makes application of DSG independent of the order and form of the finite elements as the main difference from the ANS. The DSG method has been recently used in combination with the Edge-Based Smoothed FE Method (ES-FEM) [12], as a particular meshless method [13].

The developed finite elements are ordinary based on direct application of the Mindlin plate theory, which deals with plate deflection and angles of rotation as three basic variables. In this paper a new thick plate theory is proposed, representing an extension of the issue elaborated in [14]. The main idea is to split deflection and angles of rotation in their constitutive parts, i.e. pure bending deflection and shear deflection with bending angles, and in-plane shear angles, respectively. In that way the problem is decomposed into flexural (bending and transverse shear) vibrations and in-plane shear vibrations, which can be analysed separately. Formulation of finite elements for both flexural and in-plane shear vibrations, using the standard FE procedure, is presented.

2 Basic equations of Mindlin plate theory

The Mindlin theory deals with three general displacements, i.e. plate deflection w, and angles of cross-section rotation about y and x axis, ψ_x and ψ_y, respectively. The following relations between sectional forces, i.e. bending moments, M_x and M_y, torsional moments, M_{xy} and M_{yx}, and transverse shear forces, Q_x and Q_y, and displacements via deformations are specified, [1] and [2]

$$
\begin{aligned}
M_x &= D\left(\frac{\partial \psi_x}{\partial x} + \nu \frac{\partial \psi_y}{\partial y}\right),\\
M_y &= D\left(\frac{\partial \psi_y}{\partial y} + \nu \frac{\partial \psi_x}{\partial x}\right),\\
M_{xy} &= M_{yx} = \frac{1}{2}(1-\nu)D\left(\frac{\partial \psi_x}{\partial y} + \frac{\partial \psi_y}{\partial x}\right),\\
Q_x &= S\left(\frac{\partial w}{\partial x} + \psi_x\right),\ \ Q_y = S\left(\frac{\partial w}{\partial y} + \psi_y\right),
\end{aligned}
\tag{1}
$$

where

$$
D = \frac{Eh^3}{12\left(1-\nu^2\right)},\ \ S = kGh,
\tag{2}
$$

is plate flexural rigidity and shear rigidity, respectively, h is plate thickness, k is shear coefficient, E and $G = E/\left(2\left(1+\nu\right)\right)$ are Young's and shear modulus, respectively, while ν is Poisson's ratio.

The plate is loaded with transverse inertia load and distributed inertia moments

$$
q = -\overline{m}\frac{\partial^2 w}{\partial t^2},\quad m_x = J\frac{\partial^2 \psi_x}{\partial t^2},\quad m_y = J\frac{\partial^2 \psi_y}{\partial t^2},
\tag{3}
$$

where $\overline{m} = \rho h$ and $J = \rho h^3/12$ are plate specific mass per unit area and its moment of inertia, respectively, and ρ is mass density.

Equilibrium of sectional and inertia forces, i.e. moment about y and x axis and transverse forces read

$$
\begin{aligned}
&\frac{\partial M_x}{\partial x} + \frac{\partial M_{xy}}{\partial y} - Q_x = m_x,\\
&\frac{\partial M_y}{\partial y} + \frac{\partial M_{yx}}{\partial x} - Q_y = m_y,\\
&\frac{\partial Q_x}{\partial x} + \frac{\partial Q_y}{\partial y} = -q.
\end{aligned}
\tag{4}
$$

By substituting Eqs. (1) and (3) into (4) one arrives at three differential equations of motion

$$
\frac{D}{S}\left[\frac{\partial^2 \psi_x}{\partial x^2} + \frac{1}{2}(1-\nu)\frac{\partial^2 \psi_x}{\partial y^2} + \frac{1}{2}(1+\nu)\frac{\partial^2 \psi_y}{\partial x \partial y}\right] - \left(\frac{\partial w}{\partial x} + \psi_x\right) - \frac{J}{S}\frac{\partial^2 \psi_x}{\partial t^2} = 0,
\tag{5}
$$

$$
\frac{D}{S}\left[\frac{\partial^2 \psi_y}{\partial y^2} + \frac{1}{2}(1-\nu)\frac{\partial^2 \psi_y}{\partial x^2} + \frac{1}{2}(1+\nu)\frac{\partial^2 \psi_x}{\partial x \partial y}\right] - \left(\frac{\partial w}{\partial y} + \psi_y\right) - \frac{J}{S}\frac{\partial^2 \psi_y}{\partial t^2} = 0,
\tag{6}
$$

$$
\Delta w + \frac{\partial \psi_x}{\partial x} + \frac{\partial \psi_y}{\partial y} - \frac{\overline{m}}{S}\frac{\partial^2 w}{\partial t^2} = 0,
\tag{7}
$$

where $\Delta(.) = \frac{\partial^2(.)}{\partial x^2} + \frac{\partial^2(.)}{\partial y^2}$ is the Laplace differential operator.

Eqs. (5), (6) and (7) are the well-known Mindlin equations of motion [2] and represent a starting point for further development of the Mindlin theory and its variants, with their advantages and shortcomings such as the well-known shear locking in FEM formulation. That state-of-the-art motivates further investigation of this challenging problem.

3 Development of new thick plate theory

The main idea is to split general displacements w, ψ_x and ψ_y, Figure 1a, into their constitutive parts, as shown in Figure 1, b, c and d. Total deflection consists of bending deflection and contribution of transverse shear, while the angles of plate cross-section slope are a result of rotation due to pure bending and shearing

$$w = w_b + w_s, \quad \psi_x = -\frac{\partial w_b}{\partial x} + \vartheta_x, \quad \psi_y = -\frac{\partial w_b}{\partial y} + \vartheta_y. \tag{8}$$

By introducing (8) into Eqs. (5), (6) and (7), it is possible to separate variables of two different displacement fields

$$\frac{\partial}{\partial x}\left(\frac{D}{S}\Delta w_b - \frac{J}{S}\frac{\partial^2 w_b}{\partial t^2} + w_s\right) = \frac{D}{S}\left[\frac{\partial^2 \vartheta_x}{\partial x^2} + \frac{1}{2}(1-\nu)\frac{\partial^2 \vartheta_x}{\partial y^2} + \frac{1}{2}(1+\nu)\frac{\partial^2 \vartheta_y}{\partial x \partial y}\right] - \vartheta_x - \frac{J}{S}\frac{\partial^2 \vartheta_x}{\partial t^2}, \tag{9}$$

$$\frac{\partial}{\partial y}\left(\frac{D}{S}\Delta w_b - \frac{J}{S}\frac{\partial^2 w_b}{\partial t^2} + w_s\right) = \frac{D}{S}\left[\frac{\partial^2 \vartheta_y}{\partial y^2} + \frac{1}{2}(1-\nu)\frac{\partial^2 \vartheta_y}{\partial x^2} + \frac{1}{2}(1+\nu)\frac{\partial^2 \vartheta_x}{\partial x \partial y}\right] - \vartheta_y - \frac{J}{S}\frac{\partial^2 \vartheta_y}{\partial t^2}, \tag{10}$$

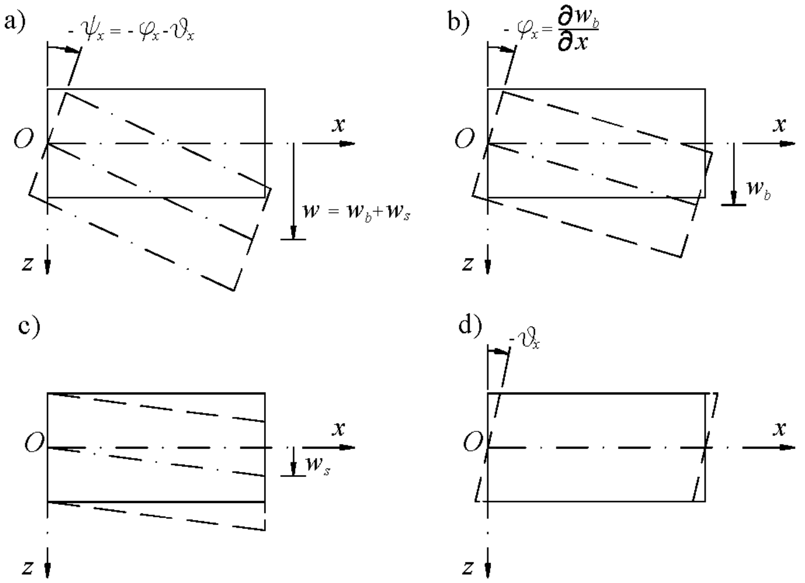

Figure 1 **Thick plate displacements, a – total deflection and rotation w, ψ_x, b – pure bending deflection and rotation w_b, φ_x, c - transverse shear deflection w_s, d – in-plane shear angle ϑ_x**

Slika 1 **Pomaci debele ploče, a – ukupni progib i kut zakreta w, ψ_x, b – progib čistog savijanja i kut zakreta w_b, φ_x, c – progib poprečnog smicanja w_s, d – kut ravninskog smicanja ϑ_x**

$$\Delta w_s - \frac{\overline{m}}{S}\frac{\partial^2}{\partial t^2}\left(w_b + w_s\right) = -\left(\frac{\partial \vartheta_x}{\partial x} + \frac{\partial \vartheta_y}{\partial y}\right). \tag{11}$$

Eqs. (9) and (10) can be presented in the form

$$\frac{\partial F\left(w_b, w_s\right)}{\partial x} = g_1\left(\vartheta_x, \vartheta_y\right), \quad \frac{\partial F\left(w_b, w_s\right)}{\partial y} = g_2\left(\vartheta_x, \vartheta_y\right) \tag{12}$$

and their integrals per x and y read $F = \int g_1 \mathrm{d}x + f(y,t) = G_1$ and $F = \int g_2 \mathrm{d}y + f(x,t) = G_2$ respectively. That implies the identity of functions G_1 and G_2, which is not possible due to structure of g_1 and g_2 in (9) and (10). The reasonable solution is that both the functions g_1 and g_2 are set to zero. Consequently, $\partial F/\partial x$ and $\partial F/\partial y$ are also zero and their integrals $F = f(y,t)$ and $F = f(x,t)$ have to be the same, i.e. $f(y,t) = f(x,t) = f(t)$. Since $f(t)$ represents rigid body motion it can be ignored in vibration analysis.

As a result of the above consideration, the following relation from Eqs. (9) and (10) is obtained

$$w_s = -\frac{D}{S}\Delta w_b + \frac{J}{S}\frac{\partial^2 w_b}{\partial t^2}. \tag{13}$$

Furthermore, by substituting Eq. (13) into (11) one arrives at differential equation for flexural vibrations

$$\Delta\Delta w_b - \frac{J}{D}\left(1 + \frac{\overline{m}D}{JS}\right)\frac{\partial^2}{\partial t^2}\Delta w_b + \frac{\overline{m}}{D}\frac{\partial^2}{\partial t^2}\left(w_b + \frac{J}{S}\frac{\partial^2 w_b}{\partial t^2}\right) = \frac{S}{D}\left(\frac{\partial \vartheta_x}{\partial x} + \frac{\partial \vartheta_y}{\partial y}\right). \tag{14}$$

Once w_b is determined, the total deflection reads, according to Eqs. (8) and (13),

$$w = w_b - \frac{D}{S}\Delta w_b + \frac{J}{S}\frac{\partial^2 w_b}{\partial t^2}. \tag{15}$$

In addition, since functions $G_1 = 0$ and $G_2 = 0$, the right-hand sides of Eqs. (9) and (10) represent the system of two differential equations for in-plane shear vibrations

$$\frac{D}{S}\left[\frac{\partial^2 \vartheta_x}{\partial x^2} + \frac{1}{2}(1-\nu)\frac{\partial^2 \vartheta_x}{\partial y^2} + \frac{1}{2}(1+\nu)\frac{\partial^2 \vartheta_y}{\partial x \partial y}\right] - \vartheta_x - \frac{J}{S}\frac{\partial^2 \vartheta_x}{\partial t^2} = 0, \tag{16}$$

$$\frac{D}{S}\left[\frac{\partial^2 \vartheta_y}{\partial y^2} + \frac{1}{2}(1-\nu)\frac{\partial^2 \vartheta_y}{\partial x^2} + \frac{1}{2}(1+\nu)\frac{\partial^2 \vartheta_x}{\partial x \partial y}\right] - \vartheta_y - \frac{J}{S}\frac{\partial^2 \vartheta_y}{\partial t^2} = 0. \tag{17}$$

In that way the system of equations with three general variables w, ψ_x and ψ_y is transformed into the system of three equations, Eqs. (14), (16) and (17), with three basic variables, i.e. pure bending deflection and in-plane shear angles w_b, ϑ_x and ϑ_y, respectively.

4 Differential equations of natural vibrations

In case of natural vibrations $w_b = W_b \sin \omega t$, $\vartheta_x = \Theta_x \sin \omega t$ and $\vartheta_y = \Theta_y \sin \omega t$, so that system of Eqs. (14), (16) and (17) is reduced to the vibration amplitudes

$$\Delta\Delta W_b + \frac{\omega^2 J}{D}\left(1 + \frac{\overline{m}D}{JS}\right)\Delta W_b + \frac{\omega^2 \overline{m}}{D}\left(\frac{\omega^2 J}{S} - 1\right)W_b = \frac{S}{D}\left(\frac{\partial \Theta_x}{\partial x} + \frac{\partial \Theta_y}{\partial y}\right), \tag{18}$$

$$\left[\frac{\partial^2 \Theta_x}{\partial x^2} + \frac{1}{2}(1-\nu)\frac{\partial^2 \Theta_x}{\partial y^2} + \frac{1}{2}(1+\nu)\frac{\partial^2 \Theta_y}{\partial x \partial y}\right] + \frac{S}{D}\left(\frac{\omega^2 J}{S} - 1\right)\Theta_x = 0, \tag{19}$$

$$\left[\frac{\partial^2 \Theta_y}{\partial y^2} + \frac{1}{2}(1-\nu)\frac{\partial^2 \Theta_y}{\partial x^2} + \frac{1}{2}(1+\nu)\frac{\partial^2 \Theta_x}{\partial x \partial y}\right] + \frac{S}{D}\left(\frac{\omega^2 J}{S} - 1\right)\Theta_y = 0. \tag{20}$$

Amplitude of total deflection according to (15) reads

$$W = \left(1 - \frac{\omega^2 J}{S}\right) W_b - \frac{D}{S} \Delta W_b. \tag{21}$$

Coefficient in the second term of (18) can be presented in a simpler form

$$\mu = 1 + \frac{\bar{m}D}{JS} = 1 + \frac{2}{(1-\nu)k}. \tag{22}$$

It is worth-while to point out that the structure of Eqs. (19) and (20) for in-plane shear vibrations is similar to that of in-plane membrane vibrations well-known in the theory of elasticity [15]

$$\frac{\partial^2 u}{\partial x^2} + \frac{1}{2}(1-\nu)\frac{\partial^2 u}{\partial y^2} + \frac{1}{2}(1+\nu)\frac{\partial^2 v}{\partial x \partial y} + \left(1-\nu^2\right)\frac{\rho}{E}\omega_m^2 u = 0, \tag{23}$$

$$\frac{\partial^2 v}{\partial y^2} + \frac{1}{2}(1-\nu)\frac{\partial^2 v}{\partial x^2} + \frac{1}{2}(1+\nu)\frac{\partial^2 u}{\partial x \partial y} + \left(1-\nu^2\right)\frac{\rho}{E}\omega_m^2 v = 0. \tag{24}$$

Both, the system of Eqs. (19) and (20), and that of Eqs. (23) and (24), deals with the same differential operators. Angles Θ_x and Θ_y correspond to membrane displacements u and v. Differences are additional moments $S\Theta_x$ and $S\Theta_y$, which are associated with inertia moments $\omega^2 J\Theta_x$ and $\omega^2 J\Theta_y$, and represent reaction of imagined rotational elastic foundation with stiffness per unit cross-section area equal to the plate shear stiffness per unit breadth, S. Hence, based on the recognized analogy, shown in Figure 2 where $K_m = 0$, plate in-plane shear response can be obtained by membrane vibration analysis performed for the same boundary conditions. Analytical solution can be found in [15, 16]. The functions of natural modes are the same in both cases, while the natural frequencies are different. Their relation arises from the equality of factors related to the function Θ_x and u, i.e. Θ_y and v, which are the same. Hence, one finds

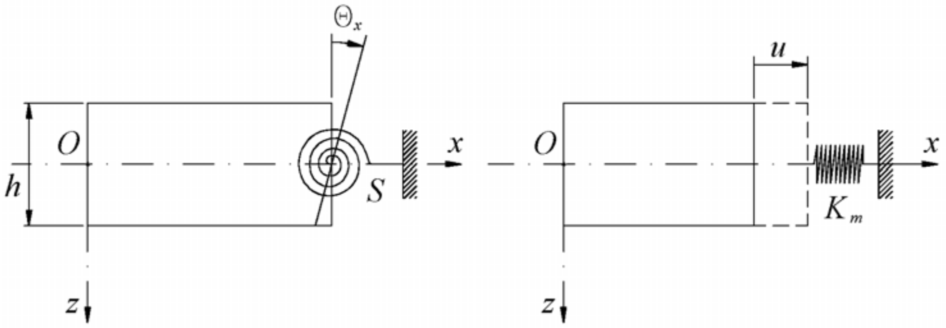

Figure 2 **Analogy between in-plane shear model and membrane model**
Slika 2 **Analogija između modela ravninskog smicanja i modela membrane**

$$\omega = \sqrt{\frac{S}{J} + \omega_m^2}. \tag{25}$$

Expression $\omega_{00} = \sqrt{S/J}$ is natural frequency of plate layers oscillating on in-plane elastic foundation (as a set of playing cards) and is obtained from Eqs. (19) and (20) for constant values of Θ_x and Θ_y. In that case disturbing function in (18) vanishes and there is no possible coupling between flexural and in-plane shear vibrations.

5 Natural vibrations of rectangular plate

In order to analyse physical background of differential equations of vibrations, a simply supported rectangular plate with aspect ratio a/b is considered. Amplitude of bending deflection and shear angles are assumed in the form of double trigonometric series

$$\begin{aligned} W_{bmn} &= A\sin\frac{m\pi x}{a}\sin\frac{n\pi y}{b}, \\ \Theta_{xmn} &= B\cos\frac{m\pi x}{a}\sin\frac{n\pi y}{b}, \\ \Theta_{ymn} &= C\sin\frac{m\pi x}{a}\cos\frac{n\pi y}{b}. \end{aligned} \tag{26}$$

Hence, total deflection w, Eq. (15), and bending moments (1) are zero at the edges, while the boundary conditions for the in-plane shear vibrations read

$$\begin{aligned} &\left.\begin{matrix} x=0 \\ x=a \end{matrix}\right\} M_{xmn}=0,\;\; \Theta_{ymn}=0, \\ &\left.\begin{matrix} y=0 \\ y=b \end{matrix}\right\} M_{ymn}=0,\;\; \Theta_{xmn}=0. \end{aligned} \tag{27}$$

By substituting (26) into (18), (19) and (20), the following system of three homogenous algebraic equations is obtained

$$\begin{bmatrix} d_{11} & d_{12} & d_{13} \\ 0 & d_{22} & d_{23} \\ 0 & d_{32} & d_{33} \end{bmatrix} \begin{Bmatrix} A \\ B \\ C \end{Bmatrix} = \begin{Bmatrix} 0 \\ 0 \\ 0 \end{Bmatrix}, \tag{28}$$

where

$$\begin{aligned} d_{11} &= c_{mn}^2 - \omega^2\mu\frac{J}{D}c_{mn} + \frac{\omega^2\bar{m}}{D}\left(\frac{\omega^2 J}{S}-1\right),\;\; d_{12}=\frac{S}{D}\frac{m\pi}{a},\;\; d_{13}=\frac{S}{D}\frac{n\pi}{b}, \\ d_{22} &= \left[\left(\frac{m\pi}{a}\right)^2+\frac{1}{2}(1-\nu)\left(\frac{n\pi}{b}\right)^2\right]+\frac{S}{D}\left(1-\omega^2\frac{J}{S}\right),\;\; d_{23}=d_{32}=\frac{1}{2}(1+\nu)\frac{m\pi}{a}\frac{n\pi}{b}, \\ d_{33} &= \left[\frac{1}{2}(1-\nu)\left(\frac{m\pi}{a}\right)^2+\left(\frac{n\pi}{b}\right)^2\right]+\frac{S}{D}\left(1-\omega^2\frac{J}{S}\right). \end{aligned} \tag{29}$$

Determinant of system (28) has to be equal to zero in order to obtain a nontrivial solution, i.e. $\mathrm{Det} = d_{11}\left(d_{22}d_{33}-d_{23}d_{32}\right)=0$. The first condition $d_{11}=0$ and the second one $d_{22}d_{33}-d_{23}d_{32}=0$ represent the frequency equation of flexural vibrations and in-plane shear vibrations, respectively. It is obvious that these two types of vibrations are not coupled. From the first condition one obtains

$$\omega_{mn}^4 - a_{mn}\omega_{mn}^2 + b_{mn} = 0, \tag{30}$$

where

$$\begin{aligned} a_{mn} &= \left(1+\mu\frac{J}{\bar{m}}c_{mn}\right)\frac{S}{J}, \\ b_{mn} &= \frac{DS}{\bar{m}J}c_{mn}^2, \\ c_{mn} &= \left(\frac{m\pi}{a}\right)^2+\left(\frac{n\pi}{b}\right)^2. \end{aligned} \tag{31}$$

The solution of (30) gives

$$\omega_{mn} = \sqrt{\frac{S}{2J}}\sqrt{1+\frac{\mu J}{\sqrt{\bar{m}D}}\Omega_{mn} - \sqrt{\left(1+\frac{\mu J}{\sqrt{\bar{m}D}}\Omega_{mn}\right)^2 - \frac{4J}{S}\Omega_{mn}^2}}, \tag{32}$$

where

$$\Omega_{mn} = c_{mn}\sqrt{\frac{D}{\bar{m}}} \tag{33}$$

is the well-known formula for the natural frequencies of the thin plate.

The second condition, $d_{22}d_{33} - d_{23}d_{32} = 0$, in expanded form reads

$$\Lambda^2 - p_{mn}\Lambda + q_{mn} = 0, \tag{34}$$

where

$$\Lambda = \frac{S}{D}\left(\frac{J}{S}\omega_{mn}^2 - 1\right), \tag{35}$$

and after some manipulation,

$$p_{mn} = \frac{1}{2}(3-\nu)c_{mn}, \;\; q_{mn} = \frac{1}{2}(1-\nu)c_{mn}^2. \tag{36}$$

The eigenvalues of Eq. (34) read

$$\Lambda_1 = c_{mn}, \;\; \Lambda_2 = \frac{1}{2}(1-\nu)c_{mn} \tag{37}$$

and one finds from (35) for natural frequencies of in-plane shear vibrations

$$\omega_{mn}^{(1)} = \sqrt{\frac{S}{D} + \frac{D}{J}c_{mn}}, \tag{38}$$

$$\omega_{mn}^{(2)} = \sqrt{\frac{S}{D} + \frac{1}{2}(1-\nu)\frac{D}{J}c_{mn}}. \tag{39}$$

Due to practical reason, a non-dimensional frequency parameter is introduced as $\lambda = \omega a^2\sqrt{\rho h/D}/\pi^2$. In that case Eqs. (38) and (39) are transformed into

$$\lambda_{mn}^{(1)} = \sqrt{12}\left(\frac{a}{\pi h}\right)^2\sqrt{6(1-\nu)k + \left(\frac{m\pi h}{a}\right)^2 + \left(\frac{n\pi h}{b}\right)^2}, \tag{40}$$

$$\lambda_{mn}^{(2)} = \left(\frac{a}{\pi h}\right)^2\sqrt{6(1-\nu)\left[12k + \left(\frac{m\pi h}{a}\right)^2 + \left(\frac{n\pi h}{b}\right)^2\right]}. \tag{41}$$

The above expressions can be also presented as $\lambda_{mn}^{(1,2)} = \sqrt{\lambda_0^2 + \left[\lambda_{mn}^{(1,2)}\right]^2}$, where the first and the second term are related to the frequency parameter of plate layers oscillations on elastic foundation and membrane vibrations, respectively. According to Eqs. (38) and (39), the membrane has two frequency spectra, with frequency ratio $1:\sqrt{(1-\nu)/2}$. On the other side, frequency squared of in-plane shear vibrations is shifted for S/J with respect to the membrane frequency squared. For longitudinal vibrations of a free bar the first solution, Eq. (40), is relevant, which gives the well-known formula for the natural frequencies $\omega_m = (\bar{m}\pi/a)\sqrt{E/\rho}$. Relative amplitudes of natural modes are determined from the second or the third equation in (28) as $B = d_{23}$ and $C = -d_{22}$, and $B = d_{33}$ and $C = -d_{32}$, respectively.

The problem of in-plane shear vibrations is also analysed in [17] in order to investigate the so-called missing modes in the spectrum of flexural plate vibrations. However, only one expression for frequency parameters is identified, which is identical to Eq. (41).

6 Rectangular finite element for flexural vibrations

A simple four node rectangular element is considered, Figure 3. The ordinary procedure for determining element properties of a thin plate is applied [18]. Bending deflection is assumed in polynomial form with the number of unknown coefficients equal to the total number of d.o.f.

$$w_b = \langle P \rangle_b \{a\}, \tag{42}$$

where $\{a\}$ is vector with terms a_i, $i = 0,1,\ldots 11$, and

$$\langle P \rangle_b = \langle 1, \xi, \eta, \xi^2, \xi\eta, \eta^2, \xi^3, \xi^2\eta, \xi\eta^2, \eta^3, \xi^3\eta, \xi\eta^3 \rangle, \tag{43}$$

where $\xi = x/a$ and $\eta = y/b$ are nondimensional coordinates. Shear polynomial, according to (13) for static analysis, reads

$$\langle P \rangle_s = -\langle 0,0,0,2\alpha,0,2\beta,6\alpha\xi,2\alpha\eta,2\beta\xi,6\beta\eta,6\alpha\xi\eta,6\beta\xi\eta \rangle, \tag{44}$$

where

$$\alpha = \frac{D}{Sa^2}, \quad \beta = \frac{D}{Sb^2}. \tag{45}$$

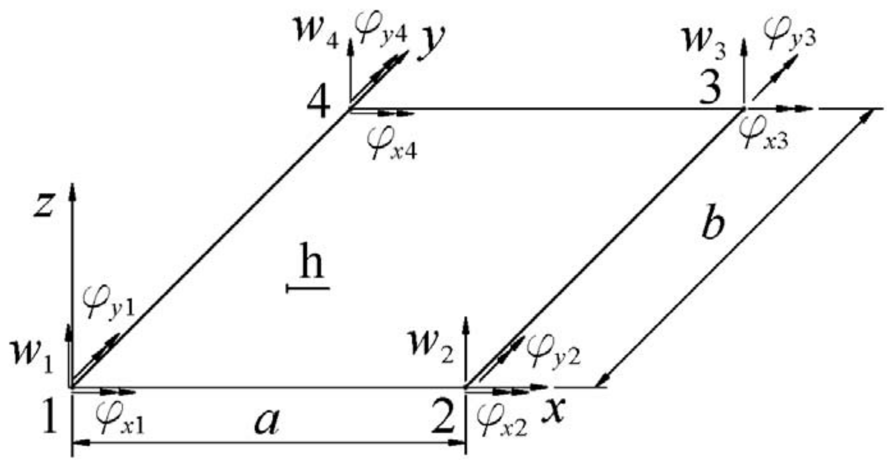

Figure 3 **Plate finite element for flexural vibrations**
Slika 3 **Konačni element ploče za fleksijske vibracije**

The total static deflection (15) can be presented in the form

$$w = \left(\langle P \rangle_b + \langle P \rangle_s \right) \{a\}, \tag{46}$$

with angles of rotation

$$\varphi_x = -\frac{1}{a}\frac{\partial \langle P \rangle_b}{\partial \xi}\{a\} = -\frac{1}{a}\langle 0,1,0,2\xi,\eta,0,3\xi^2,2\xi\eta,\eta^2,0,3\xi^2\eta,\eta^3 \rangle \{a\}, \tag{47}$$

$$\varphi_y = -\frac{1}{b}\frac{\partial \langle P \rangle_b}{\partial \eta}\{a\} = -\frac{1}{b}\langle 0,0,1,0,\xi,2\eta,0,\xi^2,2\xi\eta,3\eta^2,\xi^3,3\xi\eta^2 \rangle \{a\}. \tag{48}$$

By taking coordinate values ξ_l and η_l for each node, $l = 1,2,3,4$ into account in Eqs. (46), (47) and (48), the relation between nodal displacements and the unknown coefficients a_i is obtained

$$\{\delta\} = [C]\{a\}, \tag{49}$$

where

$$\{\delta\}=\begin{Bmatrix}\{\delta\}_1\\ \vdots\\ \{\delta\}_4\end{Bmatrix},\quad \{\delta\}_l=\begin{Bmatrix}w_l\\ \varphi_{xl}\\ \varphi_{yl}\end{Bmatrix}, \tag{50}$$

and

$$[C]=\begin{bmatrix}
1 & 0 & 0 & -2\alpha & 0 & -2\beta & 0 & 0 & 0 & 0 & 0 & 0\\
0 & 0 & \frac{1}{b} & 0 & 0 & 0 & 0 & 0 & 0 & 0 & 0 & 0\\
0 & -\frac{1}{a} & 0 & 0 & 0 & 0 & 0 & 0 & 0 & 0 & 0 & 0\\
1 & 1 & 0 & 1-2\alpha & 0 & -2\beta & 1-6\alpha & 0 & -2\beta & 0 & 0 & 0\\
0 & 0 & \frac{1}{b} & 0 & \frac{1}{b} & 0 & 0 & \frac{1}{b} & 0 & 0 & \frac{1}{b} & 0\\
0 & -\frac{1}{a} & 0 & -\frac{2}{a} & 0 & 0 & -\frac{3}{a} & 0 & 0 & 0 & 0 & 0\\
1 & 1 & 1 & 1-2\alpha & 1 & 1-2\beta & 1-6\alpha & 1-2\alpha & 1-2\beta & 1-6\beta & 1-6\alpha & 1-6\beta\\
0 & 0 & \frac{1}{b} & 0 & \frac{1}{b} & \frac{2}{b} & 0 & \frac{1}{b} & \frac{2}{b} & \frac{3}{b} & \frac{1}{b} & \frac{3}{b}\\
0 & -\frac{1}{a} & 0 & -\frac{2}{a} & -\frac{1}{a} & 0 & -\frac{3}{a} & -\frac{2}{a} & -\frac{1}{a} & 0 & -\frac{3}{a} & -\frac{1}{a}\\
1 & 0 & 1 & -2\alpha & 0 & 1-2\beta & 0 & -2\alpha & 0 & 1-6\beta & 0 & 0\\
0 & 0 & \frac{1}{b} & 0 & 0 & \frac{2}{b} & 0 & 0 & 0 & \frac{3}{b} & 0 & 0\\
0 & -\frac{1}{a} & 0 & 0 & -\frac{1}{a} & 0 & 0 & 0 & -\frac{1}{a} & 0 & 0 & -\frac{1}{a}
\end{bmatrix}. \tag{51}$$

Now, for a given nodal displacement vector, the corresponding coefficient vector $\{a\}$ can be determined from (49)

$$\{a\}=[C]^{-1}\{\delta\}. \tag{52}$$

By substituting (52) into (42) yields

$$w_b=\langle\phi\rangle_b\{\delta\},\ \langle\phi\rangle_b=\langle P\rangle_b[C]^{-1}, \tag{53a, b}$$

where $\langle\phi\rangle_b$ is the vector of the bending shape functions.

In a similar way shear deflection can be presented in the form

$$w_s=\langle P\rangle_s\{a\}, \tag{54}$$

and by employing (52) yields

$$w_s=\langle\phi\rangle_s\{\delta\},\ \langle\phi\rangle_s=\langle P\rangle_s[C]^{-1}, \tag{55a, b}$$

where $\langle\phi\rangle_s$ is the vector of the shear shape functions.

Total deflection according to (46) reads

$$w=\langle\phi\rangle\{\delta\},\ \langle\phi\rangle=\langle\phi\rangle_b+\langle\phi\rangle_s \tag{56a, b}$$

where $\langle\phi\rangle$ is the vector of the total shape functions.

Columns of inverted matrix [C] are vectors of coefficients a_i obtained for the unit value of particular nodal displacements

$$[C]^{-1}=\left[\{A\}_1\ldots\{A\}_{12}\right], \tag{57}$$

where

$$\{A\}_j^T=\left\langle a_0^j\ a_1^j\ldots a_{11}^j\right\rangle. \tag{58}$$

Bending curvatures and warping are presented in the form

$$\{\kappa\}_b = -\begin{Bmatrix} \dfrac{\partial^2 w_b}{\partial x^2} \\ \dfrac{\partial^2 w_b}{\partial y^2} \\ 2\dfrac{\partial^2 w_b}{\partial x \partial y} \end{Bmatrix}. \tag{59}$$

By substituting (53a, b) into (59) yields

$$\{\kappa\}_b = -[L]_b \{\delta\}, \ [L]_b = [H]_b [C]^{-1}, \tag{60a, b}$$

where $[L]_b$ is bending curvature matrix, and

$$[H]_b = \begin{bmatrix} \dfrac{1}{a}\dfrac{\partial^2 \langle P\rangle_b}{\partial \xi^2} \\ \dfrac{1}{b}\dfrac{\partial^2 \langle P\rangle_b}{\partial \eta^2} \\ \dfrac{2}{ab}\dfrac{\partial^2 \langle P\rangle_b}{\partial \xi \partial \eta} \end{bmatrix}. \tag{61}$$

Now it is possible to determine bending stiffness matrix by employing general formulation from the finite element method [19]

$$[K]_b = ab\int_0^1\int_0^1 [L]_b^T [D]_b [L]_b \,\mathrm{d}\xi \mathrm{d}\eta , \tag{62}$$

where

$$[D]_b = D\begin{bmatrix} 1 & \nu & 0 \\ \nu & 1 & 0 \\ 0 & 0 & (1-\nu)/2 \end{bmatrix} \tag{63}$$

is matrix of plate flexural rigidity. Furthermore, by substituting (60a, b) into (62), yields

$$[K]_b = [C]^{-T} [B][C]^{-1}, \tag{64}$$

where symbolically $[C]^{-T} = \left([C]^{-1}\right)^T$ and

$$[B] = ab\int_0^1\int_0^1 [H]_b^T [D]_b [H]_b \,\mathrm{d}\xi \mathrm{d}\eta . \tag{65}$$

By taking (61) and (63) into account, (65) can be presented in the form

$$[B] = D\left([I]_1 + \nu\left([I]_2 + [I]_3\right) + [I]_4 + 2(1-\nu)[I]_5\right), \tag{66}$$

where

$$
\begin{aligned}
[I]_1 &= \frac{b}{a^3}\int_0^1\int_0^1 \frac{\partial^2\{P\}_b}{\partial\xi^2}\frac{\partial^2\langle P\rangle_b}{\partial\xi^2}\mathrm{d}\xi\mathrm{d}\eta,\\
[I]_2 &= \frac{1}{ab}\int_0^1\int_0^1 \frac{\partial^2\{P\}_b}{\partial\xi^2}\frac{\partial^2\langle P\rangle_b}{\partial\eta^2}\mathrm{d}\xi\mathrm{d}\eta = [I]_3^T,\\
[I]_4 &= \frac{a}{b^3}\int_0^1\int_0^1 \frac{\partial^2\{P\}_b}{\partial\eta^2}\frac{\partial^2\langle P\rangle_b}{\partial\eta^2}\mathrm{d}\xi\mathrm{d}\eta,\\
[I]_5 &= \frac{1}{ab}\int_0^1\int_0^1 \frac{\partial^2\{P\}_b}{\partial\xi\partial\eta}\frac{\partial^2\langle P\rangle_b}{\partial\xi\partial\eta}\mathrm{d}\xi\mathrm{d}\eta.
\end{aligned} \tag{67}
$$

According to Eqs. (1) for Θ_x and Θ_y, and (8), the vector of shear strain accompanying bending reads

$$
\{\gamma\} = \begin{Bmatrix} \dfrac{\partial w_s}{\partial x} \\ \dfrac{\partial w_s}{\partial y} \end{Bmatrix}. \tag{68}
$$

By taking (55a, b) into account, one obtains

$$
\{\gamma\} = [L]_s\{\delta\},\ [L]_s = [H]_s[C]^{-1} \tag{69a, b}
$$

where $[L]_s$ is the shear strain matrix, and

$$
[H]_s = \begin{bmatrix} \dfrac{1}{a}\dfrac{\partial\langle P\rangle_s}{\partial\xi} \\ \dfrac{1}{b}\dfrac{\partial\langle P\rangle_s}{\partial\eta} \end{bmatrix}. \tag{70}
$$

Analogously to (64), the shear stiffness matrix is presented in the form

$$
[K]_s = ab\int_0^1\int_0^1 [L]_s^T[D]_s[L]_s\,\mathrm{d}\xi\mathrm{d}\eta, \tag{71}
$$

where $[D]_s = S\begin{bmatrix} 1 & 0 \\ 0 & 1 \end{bmatrix}$. By substituting (69a, b) into (71), yields

$$
[K]_s = [C]^{-T}[S][C]^{-1}, \tag{72}
$$

where

$$
[S] = Sab\int_0^1\int_0^1 [H]_s^T[H]_s\,\mathrm{d}\xi\mathrm{d}\eta. \tag{73}
$$

By taking (70) into account, (73) can be presented in the form

$$
[S] = S\left([I]_6 + [I]_7\right), \tag{74}
$$

where

$$
\begin{aligned}
[I]_6 &= \frac{b}{a}\int_0^1\int_0^1 \frac{\partial\{P\}_s}{\partial\xi}\frac{\partial\langle P\rangle_s}{\partial\xi}\mathrm{d}\xi\mathrm{d}\eta,\\
[I]_7 &= \frac{a}{b}\int_0^1\int_0^1 \frac{\partial\{P\}_s}{\partial\eta}\frac{\partial\langle P\rangle_s}{\partial\eta}\mathrm{d}\xi\mathrm{d}\eta.
\end{aligned} \tag{75}
$$

Finally, the complete stiffness matrix is

$$[K]=[K]_b+[K]_s=[C]^{-T}\left([B]+[S]\right)[C]^{-1}. \tag{76}$$

According to the general formulation of mass matrix in the finite element method [18], one can write

$$[M]=\bar{m}ab\int_0^1\int_0^1\{\phi\}\langle\phi\rangle\,\mathrm{d}\xi\,\mathrm{d}\eta\,, \tag{77}$$

where $\{\phi\}$ is the vector of total shape functions (56b). By taking (53b) and (55b) into account yields

$$[M]=\bar{m}ab[C]^{-T}[I]_0[C]^{-1}, \tag{78}$$

where

$$[I]_0=ab\int_0^1\int_0^1\{P\}\langle P\rangle\,\mathrm{d}\xi\,\mathrm{d}\eta\,, \tag{79}$$

and $\{P\}=\{P\}_b+\{P\}_s$, Eqs. (43) and (44).

According to definition the load vector reads [19]

$$\{F\}_q=ab\int_0^1\int_0^1\{\phi\}q\,\mathrm{d}\xi\,\mathrm{d}\eta\,. \tag{80}$$

If load is constant, by employing (53b) and (55b), yields

$$\{F\}_q=abq[C]^{-T}\int_0^1\int_0^1\{P\}\mathrm{d}\xi\,\mathrm{d}\eta\,. \tag{81}$$

Finite element equation for harmonic vibration has ordinary form $\left([K]-\omega^2[M]\right)\{\delta\}=\{F\}_q$.

7 Rectangular finite element for in-plane shear vibrations

A four node rectangular element with two shear angles per node is shown in Figure 4, with origin located in the middle of the element due to reason of simpler integration of shape function over the element surface. The element is similar to the membrane element since a thick plate layer behaves as a membrane with deformations proportional to the distance from the middle surface. Therefore, the ordinary procedure for developing of the membrane finite element is employed [20].

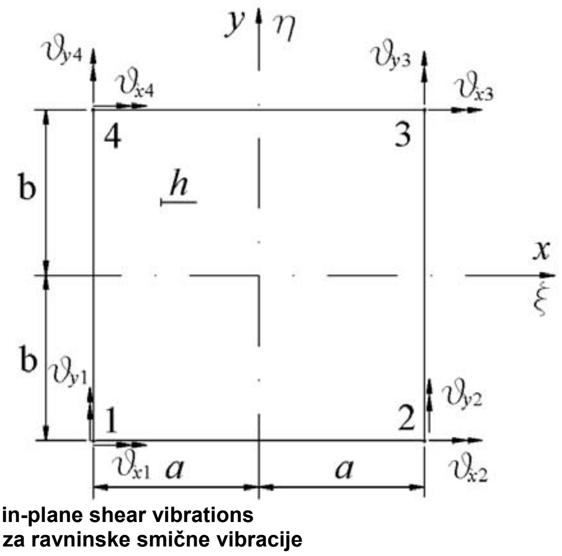

Figure 4 **Plate finite element for in-plane shear vibrations**
Slika 4 **Konačni element ploče za ravninske smične vibracije**

Shear angles are two independent variables of the same order and are assumed in the form

$$\vartheta_x = \langle P \rangle \{a\}, \quad \vartheta_y = \langle P \rangle \{b\}, \tag{82}$$

where

$$\langle P \rangle = \langle 1, \xi, \eta, \xi\eta \rangle, \tag{83}$$

$\xi = x/a$, $\eta = y/b$, $\langle a \rangle = \langle a_0, a_1, a_2, a_3 \rangle$ and $\langle b \rangle = \langle b_0, b_1, b_2, b_3 \rangle$. By taking nodal coordinates, as shown in Figure 4, into account, the nodal angles can be presented in the form

$$\{\vartheta_x\} = [C]\{a\}, \quad \{\vartheta_y\} = [C]\{b\}, \tag{84}$$

where

$$[C] = \begin{bmatrix} 1 & -1 & -1 & 1 \\ 1 & 1 & -1 & -1 \\ 1 & 1 & 1 & 1 \\ 1 & -1 & 1 & -1 \end{bmatrix}. \tag{85}$$

The unknown coefficients are obtained from (84) as

$$\{a\} = [C]^{-1}\{\vartheta_x\}, \quad \{b\} = [C]^{-1}\{\vartheta_y\}, \tag{86}$$

where in this specific case

$$[C]^{-1} = \frac{1}{4}[C]^T. \tag{87}$$

By substituting (86) into (82) yields

$$\vartheta_x = \langle \phi \rangle \{\vartheta_x\}, \quad \vartheta_y = \langle \phi \rangle \{\vartheta_y\}, \tag{88}$$

where

$$\langle \phi \rangle = \frac{1}{4}\langle P \rangle [C]^T, \tag{89}$$

is the vector of shape functions with typical term

$$\phi_i = \frac{1}{4}(1 + \xi_1\xi)(1 + \eta_i\eta), \quad i = 1,2,3,4,, \tag{90}$$

where ξ and η are nondimensional nodal coordinates.

The vector of the displacements field reads

$$\{f\} = \begin{Bmatrix} \vartheta_x \\ \vartheta_y \end{Bmatrix} = [\phi]\{\delta\},, \tag{91}$$

where $\langle \delta \rangle = \langle \vartheta_{x1}, \vartheta_{y1}, \ldots \vartheta_{x4}, \vartheta_{y4} \rangle$ is the nodal displacement vector and

$$[\phi] = \begin{bmatrix} \phi_1 & 0 & \phi_2 & 0 & \phi_3 & 0 & \phi_4 & 0 \\ 0 & \phi_1 & 0 & \phi_2 & 0 & \phi_3 & 0 & \phi_4 \end{bmatrix}, \tag{92}$$

is the matrix of shape functions.

According to (1) the deformation vector reads

$$\{\tau\} = [\Lambda]\{f\}, \tag{93}$$

where

$$
[\Lambda]=\begin{bmatrix} \dfrac{\partial}{\partial x} & 0 \\ 0 & \dfrac{\partial}{\partial y} \\ \dfrac{\partial}{\partial y} & \dfrac{\partial}{\partial x} \end{bmatrix} \tag{94}
$$

is differential operator. By substituting (91) with (92) into (93) the in-plane shear strain matrix yields

$$
[L]_p=[\Lambda][\phi]=\frac{1}{A}\begin{bmatrix} -(1-\eta)b & 0 & (1-\eta)b & 0 & (1+\eta)b & 0 & -(1+\eta)b & 0 \\ 0 & -(1-\xi)a & 0 & -(1+\xi)a & 0 & (1+\xi)a & 0 & (1-\xi)a \\ -(1-\xi)a & -(1-\eta)b & -(1+\xi)a & (1-\eta)b & (1+\xi)a & (1+\eta)b & (1-\xi)a & -(1+\eta)b \end{bmatrix} \tag{95}
$$

According to definition the stiffness matrix reads

$$
[K]_p=\frac{A}{4}\int_{-1}^{1}\int_{-1}^{1}[L]_p^T[D]_p[L]_p\,\mathrm{d}\xi\mathrm{d}\eta, \tag{96}
$$

where $A=4ab$, and $[D]_p=[D]_b$, Eq. (63). Integrals in Eq. (96) take the following values

$$
\begin{gathered}
\int_{-1}^{1}\int_{-1}^{1}(1+\xi)^2\,\mathrm{d}\xi\mathrm{d}\eta=\int_{-1}^{1}\int_{-1}^{1}(1+\eta)^2\,\mathrm{d}\xi\mathrm{d}\eta=\frac{16}{3},\\
\int_{-1}^{1}\int_{-1}^{1}(1-\xi)^2\,\mathrm{d}\xi\mathrm{d}\eta=\int_{-1}^{1}\int_{-1}^{1}(1-\eta)^2\,\mathrm{d}\xi\mathrm{d}\eta=\frac{16}{3},\\
\int_{-1}^{1}\int_{-1}^{1}\left(1-\xi^2\right)\mathrm{d}\xi\mathrm{d}\eta=\int_{-1}^{1}\int_{-1}^{1}\left(1-\eta^2\right)\mathrm{d}\xi\mathrm{d}\eta=\frac{8}{3},\\
\int_{-1}^{1}\int_{-1}^{1}(1+\xi_i\xi)(1+\eta_i\eta)\,\mathrm{d}\xi\mathrm{d}\eta=4,\\
i=1,2,3,4.
\end{gathered} \tag{97}
$$

The stiffness matrix reads $[K]_p=(D/24)[k]$, where $[k]$ is the normalized nondimensional stiffness matrix presented in Table 1, with parameters $\alpha=a/b$ and $\beta=b/a$ [21].

Table 1 **Normalized stiffness matrix for in-plane shear,** $[k]$

Tablica 1 **Normirana matrica krutosti za ravninsko smicanje,** $[k]$

$$
\begin{bmatrix}
8\beta+4(1-\nu)\alpha & 3(1+\nu) & -8\beta+2(1-\nu)\alpha & -3(1-3\nu) & -4\beta-2(1-\nu)\alpha & -3(1+\nu) & 4\beta-4(1-\nu)\alpha & 3(1-3\nu) \\
 & 8\alpha+4(1-\nu)\beta & 3(1-3\nu) & 4\alpha-4(1-\nu)\beta & -3(1+\nu) & -4\alpha-2(1-\nu)\beta & -3(1-3\nu) & -8\alpha+2(1-\nu)\beta \\
 & & 8\beta+4(1-\nu)\alpha & -3(1+\nu) & 4\beta-4(1-\nu)\alpha & -3(1-3\nu) & -4\beta-2(1-\nu)\alpha & 3(1+\nu) \\
 & & & 8\alpha+4(1-\nu)\beta & 3(1-3\nu) & -8\alpha+2(1-\nu)\beta & 3(1+\nu) & -4\alpha-2(1-\nu)\beta \\
 & & & & 8\beta+4(1-\nu)\alpha & 3(1+\nu) & -8\beta+2(1-\nu)\alpha & -3(1-3\nu) \\
 & & & & & 8\alpha+4(1-\nu)\beta & 3(1-3\nu) & 4\alpha-4(1-\nu)\beta \\
 & & & & & & 8\beta+4(1-\nu)\alpha & -3(1+\nu) \\
 \mathit{Sym.} & & & & & & & 8\alpha+4(1-\nu)\beta
\end{bmatrix}
$$

The general form of the mass matrix reads

$$
[M]_p=J\frac{A}{4}\int_{-1}^{1}\int_{-1}^{1}[\phi]^T[\phi]\,\mathrm{d}\xi\mathrm{d}\eta. \tag{98}
$$

Integrals of shape functions take the following values:

$$\int_{-1}^{1}\int_{-1}^{1}\phi_i^2 \mathrm{d}\xi \mathrm{d}\eta = \frac{1}{9},$$

$$\int_{-1}^{1}\int_{-1}^{1}\phi_i\phi_j \mathrm{d}\xi \mathrm{d}\eta = \frac{1}{18} \quad \text{for neighboring nodes,} \tag{99}$$

$$\int_{-1}^{1}\int_{-1}^{1}\phi_i\phi_j \mathrm{d}\xi \mathrm{d}\eta = \frac{1}{36} \quad \text{for diagonal nodes.}$$

By taking (99) into account, one arrives at $\left[M\right]_p = J\frac{A}{36}\left[m\right]$, where

$$\left[m\right] = \begin{bmatrix} 4 & 0 & 2 & 0 & 1 & 0 & 2 & 0 \\ & 4 & 0 & 2 & 0 & 1 & 0 & 2 \\ & & 4 & 0 & 2 & 0 & 1 & 0 \\ & & & 4 & 0 & 2 & 0 & 1 \\ & & & & 4 & 0 & 2 & 0 \\ & & & & & 4 & 0 & 2 \\ & & & & & & 4 & 0 \\ Sym. & & & & & & & 4 \end{bmatrix}, \tag{100}$$

is the normalized nondimensional mass matrix [21].

The finite element equation for in-plane shear natural vibrations reads

$$\left(\frac{D}{24}\left[k\right] + \frac{SA}{36}\left[m\right] - \omega^2\frac{JA}{36}\left[m\right]\right)\left\{\delta\right\} = \left\{0\right\}. \tag{101}$$

where the first two terms represent the total stiffness matrix consisting of the conventional stiffness and the stiffness of elastic foundation. Governing equation for the membrane element is

$$\left(\frac{D_m}{24}\left[k\right] - \omega_m^2\frac{\overline{m}A}{36}\left[m\right]\right)\left\{\delta\right\}_m = \left\{0\right\}. \tag{102}$$

where $D_m = Eh\big/\left(1-\nu^2\right)$ is membrane rigidity.

8 Illustrative examples

8.1 Simply supported square plate

Analytical solutions for frequency parameter derived in Section 5, (PS-An.) are listed in Table 2. They are compared with the present FEM solution (PS-FEM), and NASTRAN values obtained by 2D and 3D vibration analysis [22]. Boundary conditions for 3D FEM model are specified for nodes at the middle surface. PS-An. results are rigorous since they also result from direct application of the Mindlin theory. Namely, in the Mindlin theory it is possible to derive the same differential equation for the total deflection w, as homogenous part of Eq. (14) with bending deflection w_b, [2, 23]. Hence, PS-An. solution can be used as benchmark for the evaluation of numerical solutions. In the considered case NASTRAN 2D and 3D frequency parameter values are very similar, and with PS-FEM values band the exact solution. The first 9 natural modes determined by 3D FEM NASTRAN analysis are shown in Figure 5 as relief map, where sagging and hogging modal areas are noticeable. FEM mesh used in 2D and 3D NASTRAN model is 8 x 8 and 8 x 8 x 4 elements, respectively.

Table 2 **Frequency parameter $\lambda = \omega a^2 \sqrt{\rho h / D} / \pi^2$ of flexural vibrations of simply supported square plate, $h/a = 0.2$, $k = 5/6$**

Tablica 2 **Frekvencijski parametar $\lambda = \omega a^2 \sqrt{\rho h / D} / \pi^2$ fleksijskih vibracija slobodno oslonjene kvadratne ploče, $h/a = 0.2$, $k = 5/6$**

MIN* *m,n*	PS-An. [14]	PS - FEM	NASTRAN	
			2D	3D
1,1	1.768	1.803	1.682	1.651
1,2; 2,1	3.866	4.024	3.791	3.717
2,2	5.588	5.827	5.249	5.142
1,3; 3,1	6.601	7.072	6.478	6.436
2,3; 3,2	7.974	8.466	7.336	7.273
3,3	9.980	10.519	8.560	8.657

*MIN - mode identification number

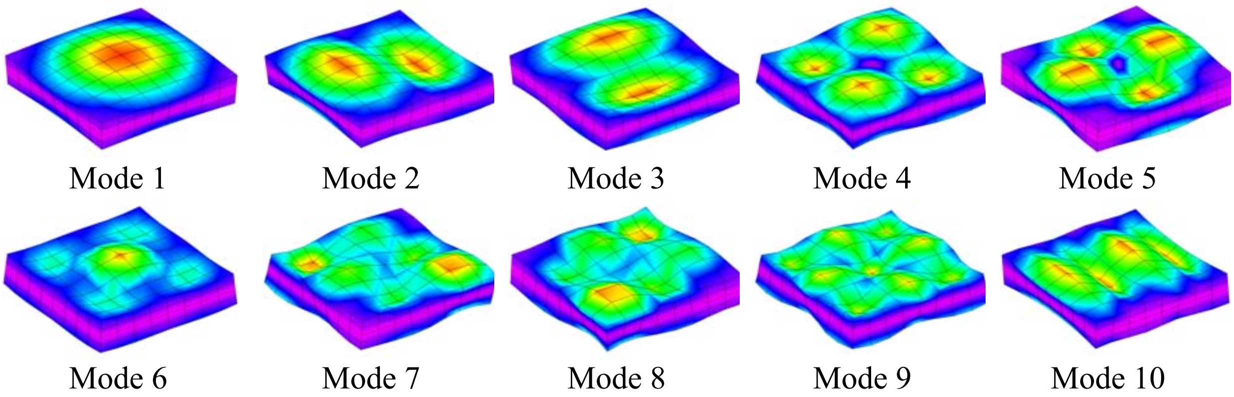

Figure 5 **Natural modes of simply supported square plate**
Slika 5 **Prirodni oblici vibriranja slobodno oslonjene kvadratne ploče**

In order to analyse plate in-plane shear vibrations the membrane eigenpairs are determined by NASTRAN, using FEM mesh 16 x 16 elements. The first 25 values of frequency parameter are listed in Table 3, while the associated natural modes are shown in Figure 6. The analytical results determined according to Section 5, PS-An. are also included in the table, with modal identification number (m,n). Most of the frequency parameters are obtained by the second root of the frequency equation (41). The remained parameter values, arising from the first root (40), are written in the brackets in Table 3. Modes of equal even numbers (m,n) are double symmetric, $(M\ 3,8,22)$, while those of odd equal numbers are antisymmetric $(M\ 9)$. The other modes for (m,n) and (n,m) have the same shape rotated for $\pi/2$. Identification of some higher modes is rather difficult since it is not only a question of (m,n) numbers, but also of ratio of integration constants B/C. The in-plane shear frequency parameters are obtained by transferring the membrane values PS-An., as states in Table 3.

Vibrations of square plate are also investigated in [17]. The in-plane frequency parameters are obtained analytically by expression (41) for the second root of the frequency equation, and the same values as those specified in the fifth column of Table 3 are reported. Hence, the values related to the first root, Eq. (40), are omitted. The obtained results are compared with those calculated by the discrete singular convolution (DSC) – Ritz method

[24], and very dense frequency spectrum is obtained. It is claimed that it holds all possible natural modes. However, the eigenpairs determined in the present analysis from the first root, Eq. (40), and presented in the brackets in the fifth column of Table 3 are not captured. Some similar values listed in brackets in the last column in Table 3 are obtained and declared as frequency parameters of coupled flexural and in-plane natural modes. Since in [17] natural modes are not presented, it is not possible to compare them with modes 8, 16 and 17 shown in Figure 6 and draw some definite conclusion.

Table 3 **Frequency parameter $\lambda = \omega a^2 \sqrt{\rho h / D} \big/ \pi^2$ of simply supported square plate, membrane and in-plane shear vibrations,** $h/a = 0.2$, $k = 5/6$

Tablica 3 **Frekvencijski parametar $\lambda = \omega a^2 \sqrt{\rho h / D} \big/ \pi^2$ slobodno oslonjene kvadratne ploče, membranske i ravninske smične vibracije,** $h/a = 0.2$, $k = 5/6$

Mode no.	MIN* m,n	Membrane		In-plane shear	
		PS – An.	NASTRAN	PS – An. transfer	DSC-Ritz method, [17]
1	0,1	3.262	3.256	16.737	16.737
2	1,0	3.262	3.256	16.737	16.737
3	1,1	4.613	4.593	17.052	17.052
4	0,2	6.532	6.482	17.664	17.664
5	2,0	6.523	6.482	17.664	17.664
6	1,2	7.293	7.222	17.963	17.963
7	2,1	7.293	7.222	17.963	17.963
8	(1,1)	(7.621)	7.753	(18.097)	(18.573)**
9	2,2	9.226	9.067	18.831	18.831
10	0,3	9.785	9.644	19.111	19.111
11	3,0	9.785	9.644	19.111	19.111
12	1,3	10.314	10.129	19.387	19.387
13	3,1	10.314	10.129	19.387	19.387
14	2,3	11.760	11.446	20.194	20.194
15	3,2	11.760	11.446	20.194	20.194
16	(1,2)	(12.326)	12.181	(20.528)	(21.235)**
17	(2,1)	(12.326)	12.181	(20.528)	(21.235)**
18			12.714		
19			12.714		
20	0,4	13.047	13.057	20.969	20.969
21	4,0	13.047	13.057	20.969	20.969
22	3,3	13.838	13.309	21.470	21.470
23			14.024		
24			14.024		
25	(2,2)	(15.593)	15.242	(22.641)	(23.504)**

*MIN - mode identification number

**Coupled flexural and in-plane modes

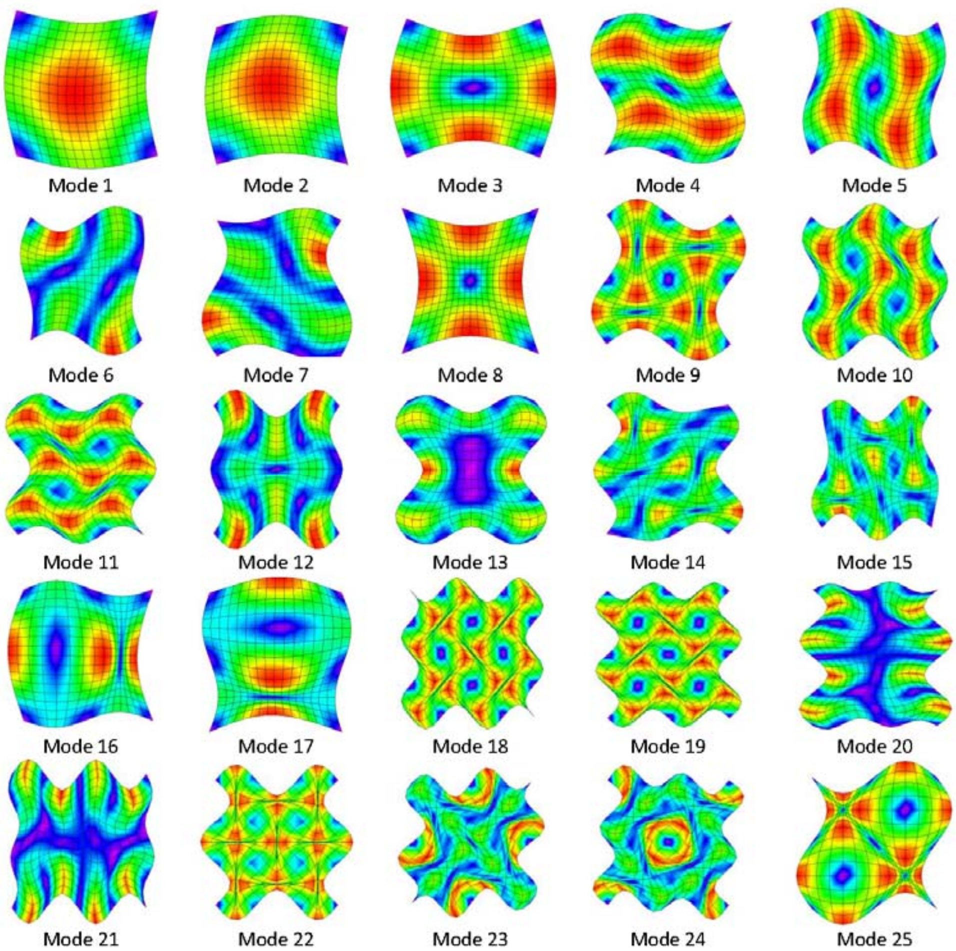

Figure 6 **Natural modes of simply supported square membrane**
Slika 6 **Prirodni oblici vibriranja slobodno oslonjene kvadratne membrane**

8.2 Clamped square plate

Vibration analysis of clamped plate is analysed by the finite element method using mesh of 8 x 8 elements. PS-FEM results and NASTRAN 2D and 3D results for flexural vibrations are listed in Table 4. In 3D FEM model all boundary nodes are fixed. The obtained results are compared with those from [25], which are obtained by the Rayleigh-Ritz method and due to high accuracy can be used for evaluation of the present solutions. As in the case of simply supported plate, PS-FEM and NASTRAN results band the referent values and discrepancies are of the same order of magnitude. The flexural natural modes determined by 3D FEM NASTRAN are shown in Figure 7.

Membrane frequency parameter determined by NASTRAN are also included in Table 4, and transferred to the values of in-plane shear vibrations according to the relation given in Section 5. Shift of parameters for about 10 is evident. The membrane natural modes, which are identical for plate layers, are shown in Figure 8.

Table 4 **Frequency parameter** $\lambda = \omega a^2 \sqrt{\rho h / D} / \pi^2$ **of clamped square plate, membrane and in-plane shear vibrations,** $h/a = 0.2$, $k = 5/6$

Tablica 4 **Frekvencijski parametar** $\lambda = \omega a^2 \sqrt{\rho h / D} / \pi^2$ **upete kvadratne ploče, membranske i ravninske smične vibracije,** $h/a = 0.2$, $k = 5/6$

Mode no.	Plate flexure				Membrane	In-plane shear
	Rayleigh-Ritz, [25]	PS - FEM	NASTRAN 2D	NASTRAN 3D	NASTRAN	Membrane transfer
1	2.687	2.724	2.657	2.758	6.115	17.518
2	4.691	4.842	4.607	4.787	6.115	17.518
3	4.691	4.842	4.607	4.787	7.118	17.893
4	6.298	6.527	5.956	6.164	8.657	18.559
5	7.177	7.640	6.942	7.240	9.593	19.013
6	7.276	7.697	7.013	7.357	9.593	19.013
7	8.515	8.989	7.786	8.096	9.747	19.091
8	8.515	8.989	7.786	8.096	11.206	19.876
9	10.013	11.031	8.985	9.342	11.378	19.974

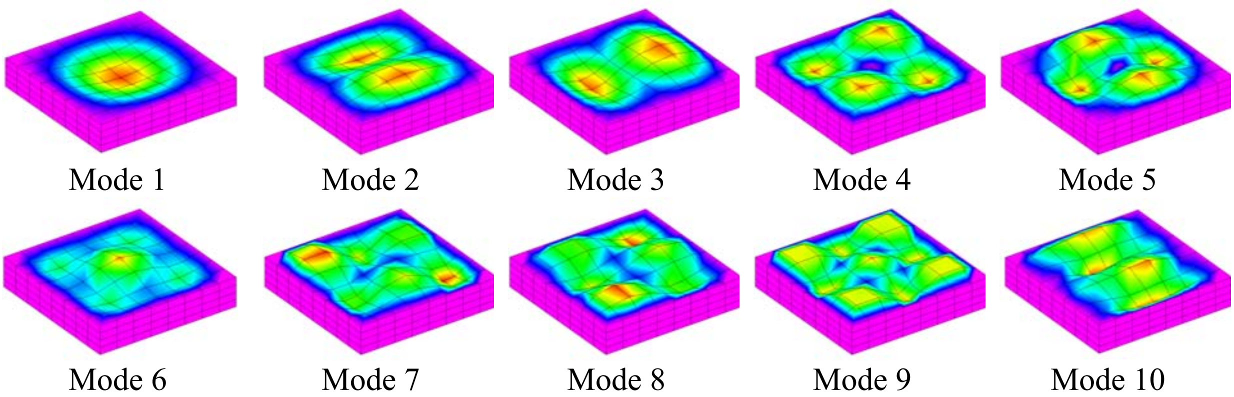

Figure 7 **Natural modes of clamped square plate**
Slika 7 **Prirodni oblici vibriranja upete kvadratne ploče**

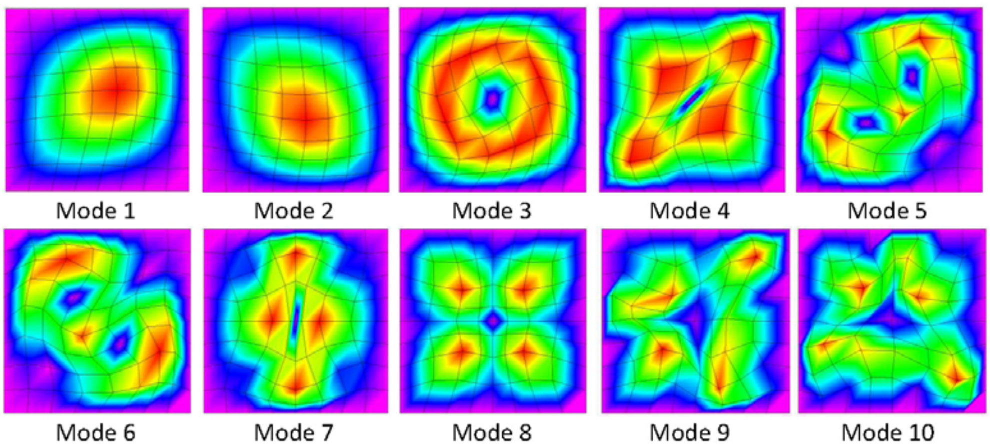

Figure 8 **Natural modes of clamped square membrane**
Slika 8 **Prirodni oblici vibriranja upete kvadratne membrane**

9 Discussion and conclusion

As elaborated in Section 2 the Mindlin thick plate theory operates with three main variables, i.e. total deflection and two slope angles of plate cross-sections. In the present theory those quantities are split into their constitutive parts, resulting in decomposed plate flexure (bending and transverse shear) and in-plane shear. These two types of vibration are related by transverse shear stiffness which appears in in-plane shear problem as stiffness of in-plane elastic foundation. Therefore, these two problems can be analysed separately. The in-plane shear task can be considered in an indirect way by using analogy with membrane equations of vibration. Natural modes of plate layers are identical to the membrane modes determined for the same boundary conditions. Natural frequencies have to be transferred from the membrane to the plate by a quite simple formula. Due to significant shift of frequency spectrum of in-plane shear vibrations with respect to that of flexural vibrations, the former might be interesting for noise analysis.

Different finite elements have been developed for thick plate analysis by taking into account total angles of rotation ψ_x and ψ_y, as single variable since their components (8) in force-strain relations (1) have the same stiffness. As shown in the present paper, bending and shear angles arise from different sources, which results with different stiffness at the finite element level. Condition of unique angles, usually interpolated by the same order polynomials as in the case of deflection, leads to the well-known shear locking since the total stiffness of thick plate cannot be reduced to the standard thin plate stiffness by decreasing plate thickness. This artificially introduced gap has been a subject of investigation for many years. Since unique solution has not been found, numerous alternative remedial procedures have been proposed with different level of success, as stated in the Introduction. Most of the procedures are based on a suitable mixed formulation of the problem. The idea consists of improving the approximated plate deflection by means of additional internal parameters, bubble modes or edge rotations. In the present finite element formulation additional rotations are introduced at the very beginning into the decoupled in-plane shear problem with physical meaning. In-plane shear is more likely membrane behaviour than plate bending and interpolation of shear slope angles is done by polynomials of lower order than the ones used for bending deflections.

Flat finite elements, comprising plate and membrane elements, are often used for modelling of thin shell structures. In a case of thick plate application, developed in-plane shear element has to be added. In that case total stiffness matrix consists of three submatrices, i.e. one for membrane deformations, one for plate flexure, and one for in-plane shear

$$[K]=\begin{bmatrix}[K]_m & & \\ & [K]_f & \\ & & [K]_{ps}\end{bmatrix}. \tag{103}$$

The matrix has to be rearranged in order to include all displacements of a node in one vector

$$\langle\delta\rangle_i=\langle u_i, v_i, w_i, \varphi_{xi}, \varphi_{yi}, \varphi_{zi}, \vartheta_{xi}, \vartheta_{yi}, \vartheta_{zi}\rangle, \tag{104}$$

where φ_{zi} and ϑ_{zi} are dummy d.o.f. In spite of the fact that bending angles of rotation and shear slope angles lie in the same planes, they cannot be unified into common d.o.f. due to different stiffness. Furthermore, the element stiffness matrix has to be transformed from the local to the global coordinate system. In that case the membrane and flexural stiffness are coupled. However, the flexural and in-plane shear stiffness matrices are not coupled in any case, because the corresponding angles always act in the same directions.

Based on the above facts, shear locking does not appear in the new finite element formulation. The developed bending and transverse shear stiffness matrices are related through parameters α and β, Eqs. (45), which depend on plate thickness squared and their values are considerably reduced for thin plates. The application of the proposed finite element procedure is illustrated in case of a simple four node rectangular plate element. The same accuracy is obtained as by sophisticated finite element incorporated in commercial software packages. That procedure can be applied for the development of more complex thick plate and shell elements with different shapes and increased number of nodes, in order to achieve higher level of accuracy in linear static and dynamic analyses.

Acknowledgment

This work was supported by a National Research Foundation of Korea (NRF) grant funded by the Korean Government (MEST) through GCRC-SOP (Grant No. 2011-0030669).

References

[1] REISSNER, E.: ‘The effect of transverse shear deformation on the bending of elastic plate’, Trans. ASME Journal of Applied Mechanics 12, 1945, p. A69-A77.

[2] MINDLIN, R.D.: ‘Influence of rotary inertia and shear on flexural motions of isotropic elastic plates’, Journal of Applied Mechanics 18 (1), 1951, p. 31-38.

[3] LIEW, K.M., XIANG, Y., KITIPORNCHAI, S.: ‘Research on thick plate vibration: a literature survey’, Journal of Sound and Vibration 180, 1995, p. 163-176.

[4] HUGHES, T.J.R.: ‘The finite element method’, Prentice Hall, New York, 1987.

[5] LEE, S.W., WONG, C.: ‘Mixed formulation finite elements for Mindlin theory plate bending’, International Journal of Numerical Methods in Engineering 18, 1982, p. 1297-1311.

[6] AURICCHIO, F., TAYLOR, R.L.: ‘A triangular thick plate finite element with an exact thin limit’, Finite Elements Analysis and Design 19, 1995, p. 57-68.

[7] LOVADINA, C.: ‘Analysis of a mixed finite element method for the Reissner-Mindlin plate problems’, Computer Methods in Applied Mechanics and Engineering 163, 1998, p.71-85.

[8] HUGHES, T.J., TEZDUYAR, T.: ‘Finite elements based upon Mindlin plate theory with particular reference to the four-node isoparametric element’, Journal of Applied Mechanics 48, 1981, p. 587-596.

[9] BATHE, K.J.: ‘Finite Element Procedures’, Prentice-Hall, Inc, New Jersey, 1996.

[10] ZIENKIEVICZ, O.C., TAYLOR, R.L.: ‘The Finite Element Method’, 5th ed. Butterworth-Heinemann, Oxford. 2000.

[11] BLETZINGER, K., BICHOFF, M., RAMM, E.: ‘A unified approach for shear-locking free triangular and rectangular shell finite elements’, Computers and structures 75, 2000, p. 321-334.

[12] NGUYEN-XUAN, H., LIU, G.R., THAI-HOANG, C., NGUYEN-THOI, T.: ‘An edge-based smoothed finite element method (ES-FEM) with stabilized discrete shear gap technique for analysis of Reissner-Mindlin plates’, Computer Methods in Applied Mechanics and Engineering 199, 2010, p. 471-489.

[13] LIU, G.R., NGUYEN-THOI, T., LAM, Y.K.: ‘An edge-based smoothed finite element method (ES_FEM) for static, free and forced vibration analyses of solids’, Journal of Sound and Vibration 320, 2009, p. 1100-1130.

[14] SENJANOVIĆ, I., VLADIMIR, N., TOMIĆ, M.: ‘An advanced theory of moderately thick plate vibrations’, Journal of Sound and Vibration, 332, 2013, p. 1868-1880.

[15] XING, Y.F., LIU, B.: ‘Exact solutions for the free in-plane vibrations of rectangular plates’, International Journal of Mechanical Sciences 51, 2009, p. 246-255.

[16] LIU, B., XING, Y.F.: ‘Exact solutions for free in-plane vibrations of rectangular plates’, Acta Mechanica Solida Sinica, Vol. 24, 2011.

[17] LIM, C.W., LI, Z.R., XIANG, Y., WEI, G.W., WANG, C.M.: ‘On the missing modes when using the exact frequency relationship between Kirchhoff and Mindlin plates’, Advances in Vibration Engineering 4 (3), 2005, p. 221-248.

[18] SZILARD, R., ‘Theories and Applications of Plate Analysis’, John Wiley & Sons, 2004.

[19] ZIENKIEVICZ, O.C.: ‘The Finite Element Method in Engineering Science’, Mc-Graw-Hill, 1971.

[20] HOLAND, J., Bell, K.: ‘Finite Element Methods in Stress Analysis’, Tapir, 1970.

[21] SENJANOVIĆ, I.: ‘Finite Element Method in Structural Analysis of Ship Structures’, University of Zagreb, 1998 (Textbook in Croatian).

[22] MSC, MSC.NASTRAN2005: ‘Installation and Operations Guide’, MSC Software, 2005.

[23] XING, Y., LIU, B.: ‘Characteristic equations and closed-form solution for free vibrations of rectangular Mindlin plates’, Acta Mechanica Solida Sinica 22 (2), 2009, p. 125-136.

[24] LIM, C.W., LI, Z.R., WEI, G.W.: ‘DCT-Ritz method for high-mode frequency analysis of thick shallow shells’, International Journal for Numerical Methods in Engineering 62, 2005, p. 205-232.

[25] LIEW, K.M., XIANG, Y. KITIPORNCHAI, S.: ‘Transverse vibration of thick plates – I. Comprehensive sets of boundary conditions’, Computers & Structures 49, 1993, p. 1-29.